



# A quick responding quartz crystal microbalance sensor array based on molecular imprinted polyacrylic acids coating for selective identification of aldehydes in body odor



Sunil K. Jha\*, Kenshi Hayashi

Kyushu University Department of Electronics Graduate School of Information Science and Electrical Engineering 744 Motoooka, Fukuoka 819-0395, Japan.

## ARTICLE INFO

### Article history:

Received 23 June 2014

Received in revised form

25 September 2014

Accepted 29 September 2014

Available online 10 November 2014

### Keywords:

QCM sensor

MIP

Body odor

Aldehydes

Pattern recognition

## ABSTRACT

In present work, a novel quartz crystal microbalance (QCM) sensor array has been developed for prompt identification of primary aldehydes in human body odor. Molecularly imprinted polymers (MIP) are prepared using the polyacrylic acid (PAA) polymer matrix and three organic acids (propenoic acid, hexanoic acid and octanoic acid) as template molecules, and utilized as QCM surface coating layer. The performance of MIP films is characterized by 4-element QCM sensor array (three coated with MIP layers and one with pure PAA for reference) dynamic and static responses to target aldehydes: hexanal, heptanal, and nonanal in single, binary, and tertiary mixtures at distinct concentrations. The target aldehydes were selected subsequent to characterization of body odor samples with solid phase-micro extraction gas chromatography mass spectrometer (SPME-GC-MS). The hexanoic acid and octanoic acid imprinted PAA exhibit fast response, and better sensitivity, selectivity and reproducibility than the propenoic acid, and non-imprinted PAA in array. The response time and recovery time for hexanoic acid imprinted PAA are obtained as 5 s and 12 s respectively to typical concentrations of binary and tertiary mixtures of aldehydes using the static response. Dynamic sensor array response matrix has been processed with principal component analysis (PCA) for visual, and support vector machine (SVM) classifier for quantitative identification of target odors. Aldehyde odors were identified successfully in principal component (PC) space. SVM classifier results maximum recognition rate 79% for three classes of binary odors and 83% including single, binary, and tertiary odor classes in 3-fold cross validation.

© 2014 Elsevier B.V. All rights reserved.

## 1. Introduction

Human body odor comprised numerous chemical components, for example, saturated and unsaturated acids, aldehydes, alcohols, ketones, hydrocarbons, amines, other nitrogen, and sulfur compounds, etc. [1–11]. The skin glands release sweat which is further intensified with the oxidation, and metabolism by characteristic bacteria, causing body odor. The composition of chemical components in body odor is perturbed by various factors such as parts of body (axilla, face, foot, scalp, groin, etc.) [2], genetic attributes [3], age [2], gender [4], diseases [5], living pattern and food [6], environmental conditions [7], and many more. Though, it has been established in several studies that each individual holds a characteristic body odor. This is the main motivation behind the growing interest in body odor studies and its practical relevance in

medical [8], security and safety [9], biometric [10], and cosmetics domains [11], etc.

Saturated and unsaturated aldehydes ( $C_3$ – $C_{11}$ ) are amongst the main established chemical components of human body odor, and documented in numerous studies [12–19]. It is found in body odor samples collected from skin odor [12–14], axillary sweat [15], breath odor [16], scalp and head odor, [17,18], feet odor [19], etc. Haze et al. [12] have noticed the presence of several saturated aldehydes such as hexanal, heptanal, octanal, nonanal, decanal, and unsaturated aldehyde (2-nonenal) in skin odor originated from oxidation of non saturated fatty acids. Authors have established 2-nonenal as the ageing biomarker chemical in body odor. Bernier et al. [13,14] have also confirmed the existence of short chain aldehydes (hexanal, heptanal, octanal, nonanal, decanal, and undecanal) along with other chemicals in skin odor analysis. Munk et al. [15] have found 4-heptenal, octanal, 2-nonenal, 2, 6-nonadienal, 2, 4-nonadienal, 2, 4-decadienal, etc. as primary chemical components in washed clothes containing axillary sweat odor. Martinez-Lozano [16] et al. have reported the presence of aldehydes besides other chemical components in breath odor analysis. Goetz et al. [17] have identified aldehydes as well other volatile

\* Corresponding author. Tel.: +81 092 802 3629; fax: +81 092 802 3629.

E-mail addresses: [drsniljha@o.ed.kyushu-u.ac.jp](mailto:drsniljha@o.ed.kyushu-u.ac.jp), [sdrsnil76@gmail.com](mailto:sdrsnil76@gmail.com) (S.K. Jha).

organic compounds in analysis of scalp and hair odor. Kubota et al. [18] have also recognized valeraldehyde and heptanal in head odor analysis. Dormont et al. [19] have investigated the volatile chemicals in feet odor and confirmed the existence of aldehydes such as hexanal, octanal, nonanal, decanal, undecanal, and tridecanal, etc.

Analytical methods have been widely used for characterization and in determination of quantitative as well qualitative chemical composition of body odor such as: headspace gas chromatography-mass spectrometer (HS-GC-MS) [12,17,18], thermal desorption (TD)-GC-MS [13,14], high resolution (HR)-GC-MS [15], atmospheric pressure ionization mass spectrometer (API-MS) [16], solid-phase micro-extraction (SPME)-GC-MS [19–22], GC with flame photometric detection (FPD) [23], GC Fourier transform infrared spectroscopy (FTIR) [24], etc. It is evident from the literature survey that GC-MS is the most efficient and extensively used analytical method for body odor research. Earlier methods are capable in laboratory based examinations; however there are certain factors (large size, long technical process and analysis time, cost, etc.) which restrain their outside applicability. These restrictions result the need of a device that can be used for real-time assessment of body odor. Since last few years, chemical sensors including metal oxide semiconductor (MOS), fluorescent imaging (FI), quartz crystal microbalance (QCM), conducting polymer composite (CPC), and surface acoustic wave (SAW), etc are being researched for the recognition of volatile organic chemicals (VOCs) in body odor [8, 20, 22, 25–28]. Though, currently limited research reports are available in literature based on application of chemical sensors for body odor evaluation. Multifarious combination of VOCs in body odor, low vapor pressure, and occurrence of external interfering chemicals necessitate the development of fast and reversible, highly sensitive, selective, and stable chemical sensors in body odor analysis. This is the main motivation behind the present study.

Compared to other chemical sensors, QCM is a simple, low cost, small size, and highly sensitive gravimetric sensor based on piezoelectric effect. A chemo selective layer is coated for vapor sorption over the surface of QCM resonator. Its frequency change is found in proportion to the mass loading according to Sauerbrey equation [29]. Application of QCM sensor array in food quality assessment, medical and drug discovery, forensic and for the development of biomimetic system, biosensors, etc have been reported in literature [30–32]. Though at present scenario, there is a need for further improvement in selectivity, reproducibility, signal to noise ratio and diminishment in drift, and complications of manufacturing process of QCM sensor [33]. Amongst these selectivity is one of the key factors for the successful real time operation, which is determined by the coating material over QCM surface. Several research groups are working for the development of novel selective materials by using polymers, nano-materials, gas chromatographic stationary phases, ionic liquids, bio-materials, etc and its optimal selection [27, 31–36]. Besides these, recently a new technique for the development of highly chemo selective polymer as surface coating material of QCM sensor has been invented, named as molecular imprinting (MI) [31, 37–42]. MI is the most effective technique for increasing the selectivity of polymer in which artificial cavities are formed inside the original polymer matrix by adding target or other chemical molecules with some cross linker. After that target molecules are removed from the host polymer matrix by simple (heating, washing, etc.) or using special chemical protocol. This procedure generates target molecules specific non-covalent binding sites inside the host polymer. Patterned host polymer is referred as molecular imprinted polymer (MIP). It combines the high selectivity feature of polymer and sensitivity of QCM resonator when coated over surface. The MIP coated QCM sensor is employed for real time sensing applications [38–42]. Percival et al. [38] have prepared MIP using the monomer methacrylic acid (MAA) and

cross-linkers ethylene glycol dimethacrylate (EDMA) and trimethylolpropane trimethacrylate (TRIM). Prepared MIP is coated over QCM surface for detection of terpenes (sensitivity 200 ppb) in liquid phase. Matsuguchi et al. [39] have developed MIP coated QCM sensors (high response time 60 min) for the detection of toluene and p-xylene. MIP is prepared with target molecules, methyl methacrylate monomer using cross-linking polymerization method. Some latest studies based on MIP-QCM sensors are as follows: Gultekin et al. [40] have proposed methacrylamido-antipyrene-iron (III) [MAAP-Fe(III)] as metal-chelating monomer based MIP for the identification of caffeic acid found in plants (detection limit 7.8 nM); Bakas et al. [41] have employed acrylamide based MIP for the removal of fenthion insecticide from olive oil (detection limit  $5 \mu\text{g L}^{-1}$ ); Yola et al. [42] have used tobramycin (TOB) imprinted poly (2-hydroxyethyl methacrylate-methacryloylamidoglutamic acid) based QCM sensor for the determination of TOB in food samples (milk, chicken, egg, etc.).

Although in last few years, MIP-QCM sensors have been employed for chemical vapor sensing in several applications, we hardly noticed any report for the detection of aldehyde odors (which is amongst the major chemical components of body odor) in single, binary, and tertiary mixture. Present study is succession of our earlier research [22] based on polyacrylic acid (PAA) and three template molecules: propenoic acid, hexanoic acid, and octanoic acid based MIP coated QCM sensor array for the identification of organic acids in single and binary mixtures. We have employed similar MIPs in present study as used in [22] for coating of three QCM sensors also an additional QCM is included as reference (coated with non-MIP PAA). The organic acids are highly polar chemical compounds due to strongly polarized carbonyl (C=O) and hydroxyl (O-H) groups. Consequently they easily interact through strong hydrogen bonding with alike molecules capable in h-bonding with greater strength than other organic compounds such as aldehydes, alcohols, amines ketones, esters, etc. This is the reason for selecting organic acids as template molecules in MIPs formation for aldehydes target molecules detection. Another objective is to develop PAA-MIP-QCM sensor array capable for the detection of chemicals from multiple functional groups such as acids, aldehydes, alcohols, etc Four element QCM sensor array was exposed to three target chemicals: hexanal, heptanal, nonanal, and their binary and tertiary mixtures at distinct concentrations. The dynamic response of sensors was measured for assessment of response time, sensitivity and repeatability. Also the static sensor array response was processed with principal component analysis (PCA) for symbolic recognition of odors in feature space and support vector machine (SVM) classifier for quantitative identification. Target aldehydes were selected after confirming their presence in body odor samples. For that purpose body odor samples are characterized using SPME-GC-MS method.

## 2. Experimental

### 2.1. GC/MS characterization of body odor

We have obtained consent from the Clinical Trials Committee of Department of Electrical Engineering, Kyushu University, Japan for human body odor detection experiments. Body odor samples were collected from the two persons (male and female). Cotton pads were used to collect the body odor samples from different parts of body including the left and right axilla, and left and right foot. The samples were collected in two different conditions of body: (a) working condition in day (sampling time 4 h), and (b) in relaxing condition of body in night (sampling time 8 h). In this way, total sixteen samples were collected (2 person  $\times$  4 body

parts  $\times$  2 conditions). After sample collection each of the cotton pads were cut into four parts resulting sixty four samples. In which each of the sixteen samples were analyzed with the GC–MS at the interval of a day, with objective to examine the change in body odor composition, due to the bacterial activity. Cotton pads were capped in cleaned glass vials and stored at fix temperature (38 °C). Previous to GC–MS analysis, each of the samples was encapsulated in SPME cells. CAR/DVB on PDMS fiber was used (temperature 70 °C, and heating time 30 min) to vaporize the odor molecules. GC–MS (Shimadzu QP2010, Japan) was used to characterize the composition of body odor (analysis time 55 min).

## 2.2. Chemicals and instruments

Hexanal, heptanal, nonanal, propenoic acid, hexanoic acid, octanoic acid, ethanol, hydrochloric acid, PAA polymer, and other chemicals were purchased from Sigma Aldrich, Japan, and they were utilized without further refinement. Structure of host polymer and three target chemicals are given in Fig. 1(a)–(d) respectively. Four quartz crystals (9 MHz AT-cut) fixed between Au electrodes purchased from Seiko EG & G, Japan were used for sensing purpose. The variation in frequency ( $\Delta f$ ) of QCM due to mass loading after chemical vapor exposure can be determined by Sauerbrey relation [29]

$$\Delta f = \frac{-2f_0^2 \Delta m}{A\sqrt{\mu \times \rho}} \quad (1)$$

where  $f_0$  is the fundamental resonant frequency of quartz crystal, and  $\mu$  is the shear modulus of quartz,  $\rho$  is the density of quartz, and  $A$  is the gold electrode coated area of QCM. Four cylindrical crystal holders were used to fix the QCM sensors with a common sensing chamber. Holders were also connected with the QCM analyzer (QCA-922) purchased from Seiko EG & G, Japan to read out the sensor response. The response of QCM sensors was recorded in CF-R4 computer using WinQCM software for further analysis.

## 2.3. MIP films preparation and coating

We have prepared three MIP films using the following procedures: (I) 250 mg of PAA was dissolved in 5 ml of ethanol in three different tubular glass vials; (II) 10  $\mu$ L of template molecules (propenoic acid, hexanoic acid, and octanoic acid) were injected using micro-syringe purchased from Nichipet Ex, Japan in three solutions respectively; (III) Finally 25  $\mu$ L of hydrochloric acid was added in each solution. Thereafter each solution was stirred for 6 h constantly. The prepared PAA–MIPs were dropped (5  $\mu$ L of each) on one side of QCMs surface, subsequently using the spin coating method (coating time 30 s at 500 rpm). Coating thickness is calculated using the mass loading of QCM and Eq. (1). It is of few hundred nm also validated by Mirmohseni et al. [43] under

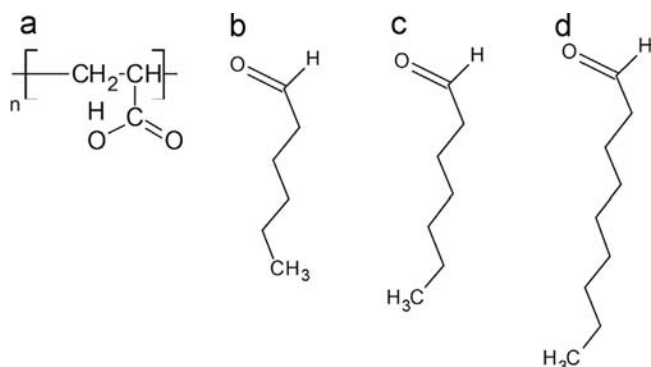


Fig. 1. Chemical structures of (a) polyacrylic acid (PAA) polymer, (b) hexanal, (c) heptanal, and (d) nonanal.

similar coating conditions. One QCM is coated with pure PAA, that is, non-MIP for reference. After that, four QCMs were dried inside a vacuum oven for 24 h at 40 °C. It assists in dislodging template molecules from the host polymer and to dry the MIP layer. Schematic diagram and real pictures of MIP–QCM sensing system are given in Figs. 2–3.

## 2.4. Vapor generation and response measurement of sensors

Pyrex glass bottles of 100 ml cleaned with inert nitrogen and connected with 100% gas tight microfluidic cap were used for vapor generation and collection of aldehydes odor. Aldehyde liquid was dropped over a cotton paper (of size 20  $\times$  12 cm) inside the glass bottle using micro-syringe. The glass bottle is connected with the two Teflon tubes, first for way in of diluting gas (pure dry air), and second for passage of generated target vapors (Figs. 2 and 3). Target aldehyde odors were generated by passing pure dry air for 15 s in glass bottle. QCM sensors are highly sensitive for humidity, which can influence its sensing. Effect of humidity can be reduced either in sensing system with proper selection of coating material, or during response processing. For instance, Sun et al. [44] have developed polypyrrole coated QCM sensor for low humidity sensing; artificial neural network (ANN) method is used for drift compensation due to humidity by Mumykmaz et al. [45]. In present research the effect of humidity was reduced by using the clean dry air as dilution gas during the odor generation, using inert nitrogen for cleaning the odor collecting glass bottles. As well the preprocessing methods and PCA for data processing reduce the noise content in sensor signal due to humidity and other interferences. Air is passed through mixture of carbon molecular sieve (adsorb humidity) and activated carbon (filter other odor molecules) inside a glass chamber to produce clean dry air (Fig. 2). Total 18 different concentrations of single aldehyde odor were generated by injecting target liquid 5–30  $\mu$ L (5  $\mu$ L in each step) on the cotton paper placed inside the glass bottle. This process results six concentrations of each aldehydes odor. Beside the single aldehyde odor, we have also generated the blend odor using the binary and tertiary mixtures of three aldehydes. With the three feasible combinations of binary mixtures of aldehydes (hexanal+heptanal, heptanal+nonanal, and hexanal+nonanal) total 108 concentrations (36 for each binary mixture) were generated. For instance 36 binary odors for mixture of hexanal and heptanal were produced by injecting the distinct amount of two aldehydes in glass bottle, in following steps: (I) 5  $\mu$ L of hexanal and 5–30  $\mu$ L of heptanal (5  $\mu$ L in each step), (II) 10  $\mu$ L of hexanal and 5–30  $\mu$ L of heptanal, (III) 15  $\mu$ L of hexanal and 5–30  $\mu$ L of heptanal, (IV) 20  $\mu$ L of hexanal and 5–30  $\mu$ L of heptanal, (V) 25  $\mu$ L of hexanal and 5–30  $\mu$ L of heptanal, and (VI) 30  $\mu$ L of hexanal and 5–30  $\mu$ L of heptanal. Each step produces six different concentrations of binary odor. The tertiary mixture of aldehydes (hexanal+heptanal+nonanal) odor were generated in subsequent ways: (I) 5  $\mu$ L of hexanal+5  $\mu$ L of heptanal and 5–30  $\mu$ L of nonanal (5  $\mu$ L in each step, this generates six different concentrations), (II) 5  $\mu$ L of hexanal+5  $\mu$ L of nonanal and 10–30  $\mu$ L of heptanal (5  $\mu$ L in each step, this generates five different concentrations), (III) 5  $\mu$ L of heptanal+5  $\mu$ L of nonanal and 10–30  $\mu$ L of hexanal (5  $\mu$ L in each step, this generates five different concentrations). Thus total 16 concentrations of tertiary odor were generated. The generated concentrations were exposed to the 4-element QCM sensor array inside the sensing chamber for response measurement. QCM sensor array response was measured for 18 distinct vapor concentrations of single aldehyde odor, 108 concentrations of binary odors, and 16 concentrations of tertiary odors. The exposure time for target odors was set to 15 s and baseline response of sensor was achieved by passing pure dry air for next 15 s. Response of each sensor was measured for 90 s (3 response cycles). Fig. 4(a)–(d) represent the response of non MIP–PAA (S1), propenoic acid template based PAA–MIP (S2), hexanoic acid template based PAA–MIP (S3), and octanoic acid template based PAA–MIP coated QCM

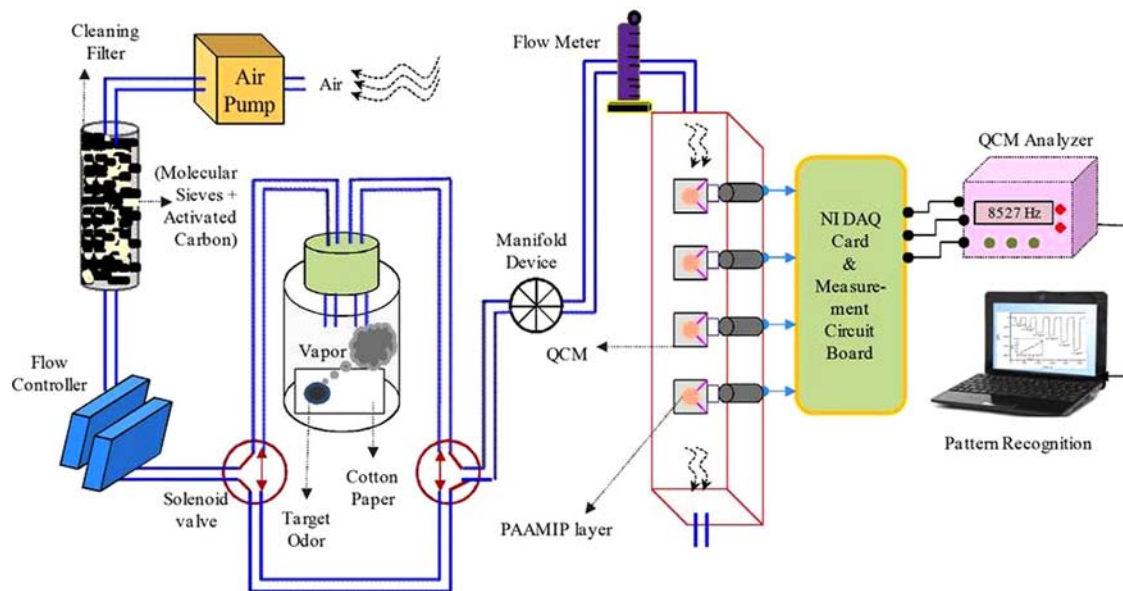


Fig. 2. Schematic diagram of 4-element QCM sensor array based odor recognition system.

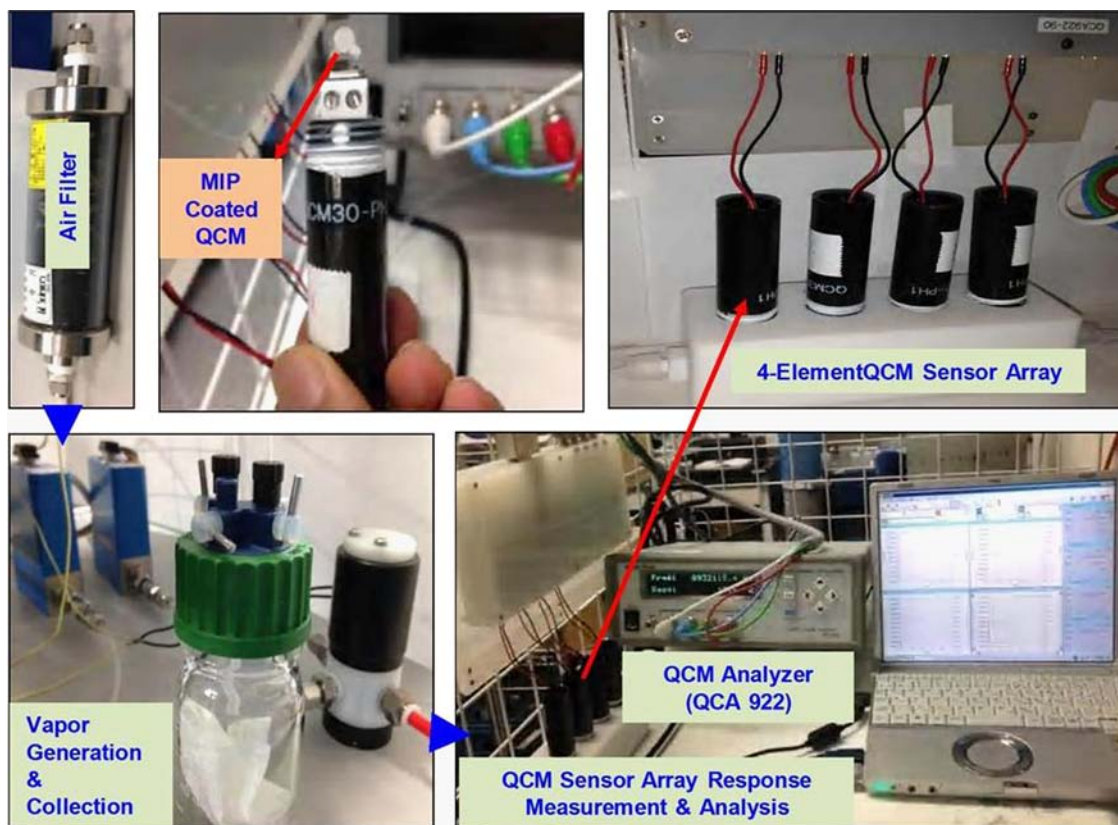


Fig. 3. Real set up of 4-element QCM sensor array.

sensors (S4) to the nonanal vapors (5  $\mu$ L in sampling vial) respectively. Response of four sensors to binary mixture of hexanal and nonanal (5+5  $\mu$ L) is given in Fig. 5 (a)–(d). Fig. 6 (a)–(d) present the response of four sensors to the tertiary mixture of hexanal+heptanal+nonanal (5+5+5  $\mu$ L).

The steady sensor response was defined as  $\Delta f = (f_b - f_v)$  using the transient sensor signal (Figs. 4–6). To reduce the noise effects due to fluctuations in transient sensor signal, baseline frequency ( $f_b$ ) was defined as average frequency of QCM in between 1<sup>th</sup>–15<sup>th</sup>

s; similarly frequency due to vapor adsorption ( $f_v$ ) was defined as average frequency of QCM in between 16<sup>th</sup>–30<sup>th</sup> s in first measurement cycle. According to the types of odor (single, binary, and tertiary), three dynamic sensor array response matrices were defined using the transient sensor signal in first measurement cycle: (a) for single aldehyde  $F_s(18 \times 4)$  (response of 4 sensors to 18 concentrations), (b) for binary mixtures of aldehyde  $F_b(108 \times 4)$  (response of 4 sensors to 108 concentrations), and (c) for tertiary mixture of aldehyde  $F_t(16 \times 4)$  (response of 4 sensors to 16

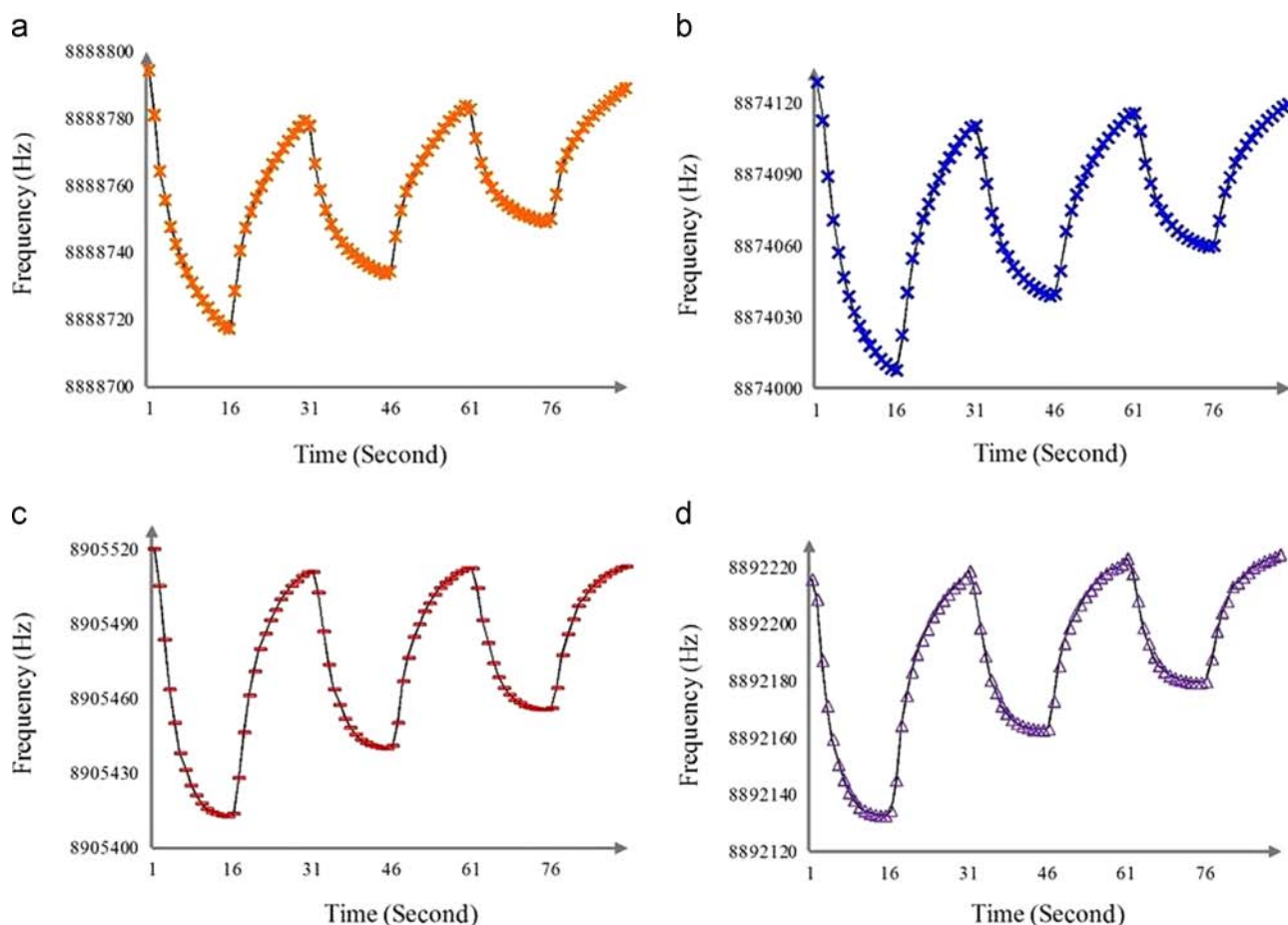


Fig. 4. Response of QCM (a) sensor (S1), (b) sensor (S2), (c) sensor (S3) and (d) sensor (S4) to nonanal vapors (5  $\mu$ L in glass bottle).

concentrations). The transient sensor response for IInd and IIIrd cycles was not used in data analysis, due to low value of reproducibility (high baseline drift).

## 2.5. Sensors response processing methods

### 2.5.1. Pre-processing

In the first step of data processing in which each of the dynamic sensor array response matrices defined in earlier section was preprocessed with the logarithmic scaling followed by the auto-scaling [46,47]. Preprocessing assists in reducing noise content as well impact of sensor on analysis outcomes. Logarithmic scaling was implemented on sensor array response matrix as:  $F \leftarrow \log(F)$ . Subsequent to logarithmic scaling, autoscaling was implemented in two steps: mean centering followed by the variance normalization along the sensors.

### 2.5.2. PCA

Next sensor array response was processed with the unsupervised linear feature extraction method PCA. Basically, it is a transformation of sensors response from measurement space to feature space with objective to minimize the correlation amongst the sensors response and maximize the variance. After that sensors response was projected along the principal axes having higher eigenvalues, to visualize the odors in two or three dimensional principal component (PC) space as well to reduce the noise content by discarding the PC directions of lower variance. In

present study there are four sensors, we discarded the fourth PC direction and used scores for first three PC directions for qualitative identification of odors in PC space and further quantitative identification by SVM classifier. Complete mathematical description of PCA method can be seen in [48,49]. The 'stats' package [50] of open source language 'R' was used in PCA analysis.

### 2.5.3. SVM

In last stage of sensors response processing, SVM classifier was employed using the PC scores as input to predict the class of odor (single, binary, or tertiary). It is a supervised classification method, proposed by Vapnik [51], and reviewed in [52]. Class identification is executed in two steps: training followed by validation. Multiclass SVM is an elaborated form of binary class SVM, in which an ideal partitioning hyperplane was formulated using the training data set, thereafter a class opinion function was decided on the basis of hyperplane equation. Quadratic programming (QP) is used to maximize the interclass margin which is measured using the data points nearby hyperplane (support vectors). Kernel functions were used in QP to reduce computation time and complexity. In multiclass identification, the training data set was divided into different groups of binary classes and SVM is trained with each. To decide class of unknown sample, first it is classified with each of the binary class trained SVM, then final class is decided on the basis of majority voting. SVM was implemented using the 'e1071' package [53] of 'R' program. Analysis flow chart for sensors response processing is given in Fig. 7.

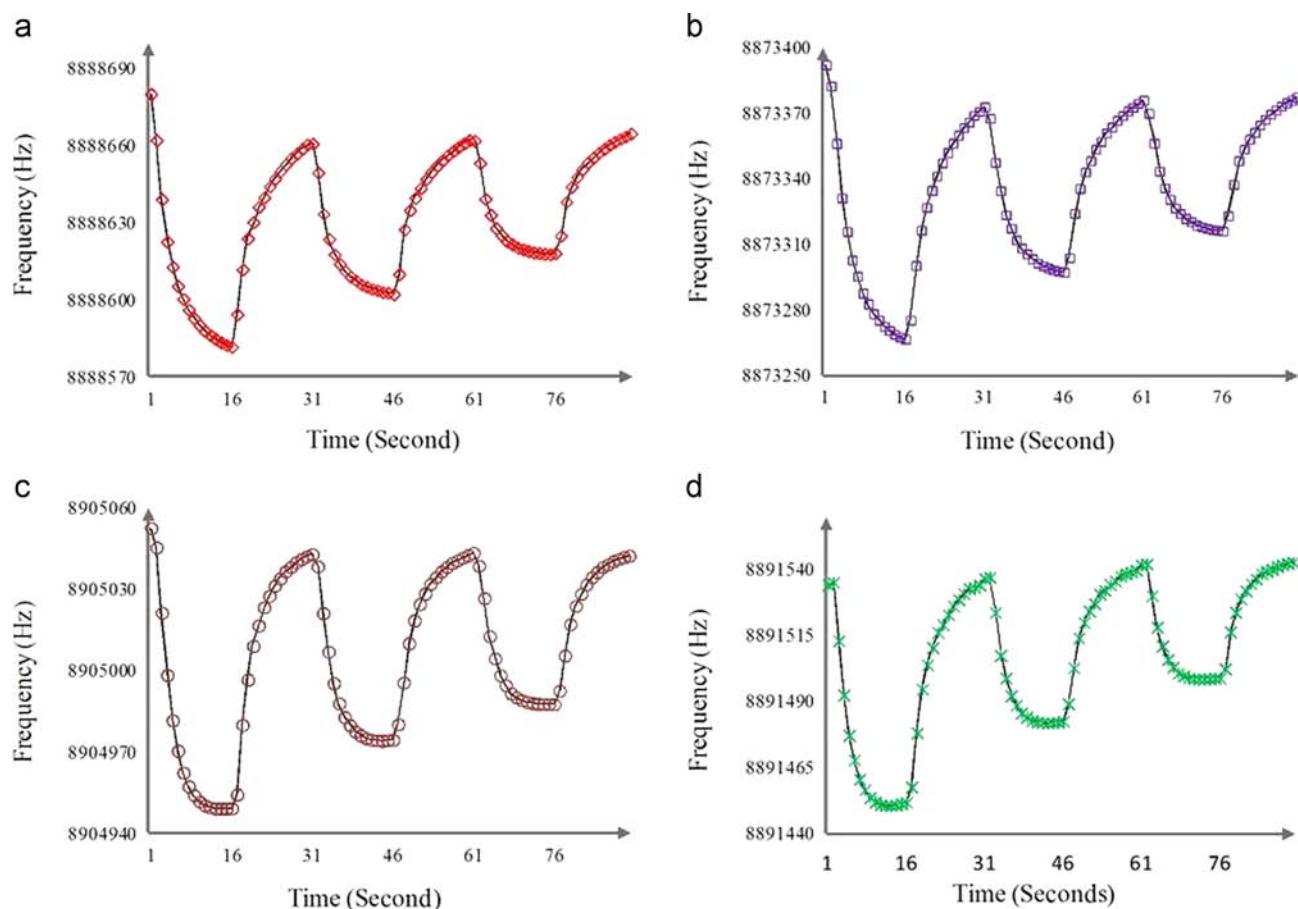


Fig. 5. Response of QCM (a) sensor (S1), (b) sensor (S2), (c) sensor (S3), and (d) sensor (S4) to binary mixture of hexanal and nonanal (5+5  $\mu$ L in glass bottle).

### 3. Results and discussions

#### 3.1. Body odor characterization result

Fig. 8 presents the characteristic GC–MS spectra for right male axilla odor in resting condition of body on first day. For body odor composition assessment 50 peaks from the GC–MS spectra were selected. Four saturated aldehydes: hexanal, heptanal, nonanal, and decanal as well as two unsaturated branched aldehydes: 2-nonenal and linal (butyl phenyl methyl-propional) were identified in GC–MS spectra of body odor. Amongst these nonanal (peak no. 14) has highest peak area 5.15% and height 7.61%. For rest of the aldehydes the peak area and height values are: 1.7% and 0.98% for hexanal (peak no. 25), 0.51% and 0.49% for heptanal (peak no. 44), 3.87% and 5.42% for decanal (peak no. 47), 0.61% and 0.85% for 2-nonenal (peak no. 49), and 0.64% and 0.71% for linal (peak no. 49) respectively. Both the saturated and unsaturated aldehydes were identified amongst the major chemical components of body odor samples collected from axilla, foot of male and female in rest condition of body (Table 1). Consequently, they can be used as biomarker chemical in body odor recognition and differentiation. Besides the aldehydes other chemical components were also identified in body odor samples such as: diethyl phthalate (peak no. 46) area 10.74%, height 13.17%, 3-hydroxy, 2-butanone (peak no. 10) peak area 5.81%, height 5.02%, 6-methyl, 5-hepten-2-one (peak no. 12) area 2.82%, height 3.74%, acetic acid (peak no. 15) area 12.16%, height 7.18%, 2-methyl-butanoic acid (peak no. 29) area 9.79%, height 5.97%, oxacyclohexadecane (peak no. 46) area 1.13%, height 1.82%, etc.

#### 3.2. Sensor array response analysis to single aldehyde odors

Passing aldehyde odor to the sensor chamber causes chemical vapor sorption in polymer layer over the QCM surface, and hence due to mass change an effective frequency change is observed. The vapor sorption in chemoselective polymer layer over the QCM surface is due to some basic non-covalent interactions including (i) the hydrogen bonding between -CHO group of aldehydes and -COOH group PAA polymer as represented in Fig. 9(a)–(c), (ii) dipole-dipole interactions, and (iii) Van der Waals interactions. Hydrogen bonding is the established interaction amongst other possible interactions which causes reproducibility characteristics of QCM sensors response to aldehyde odors. Each QCM sensor responds well to the aldehyde odor, though the average sensors response to the nonanal vapors is greater than the heptanal and hexanal vapors (Table 2). Moreover the sensors response to heptanal vapors is greater than the hexanal vapors. Performance of sensors pursue the sequential order: hexanoic acid template MIP based sensor S3 is better than propenoic acid template MIP based sensor S2 followed by non-MIP based sensor S1 and octanoic acid template MIP based sensor S4 (Fig. 4(a)–(d)). This is due to the size effect of donors and acceptors on the strength of hydrogen bonds between the target aldehyde molecules and MIPs (Fig. 9). Large size of octanoic acid template compared to other template molecules is responsible for weaker hydrogen bonding between the MIPs and target aldehyde molecules and hence low response of sensor (S4). Low vapor pressure of nonanal (0.53 mm Hg at 25 °C) compares to heptanal (3.84 mm Hg at 25 °C) and hexanal (11.3 mm Hg at 25 °C) does not influence the MIP-QCM sensors

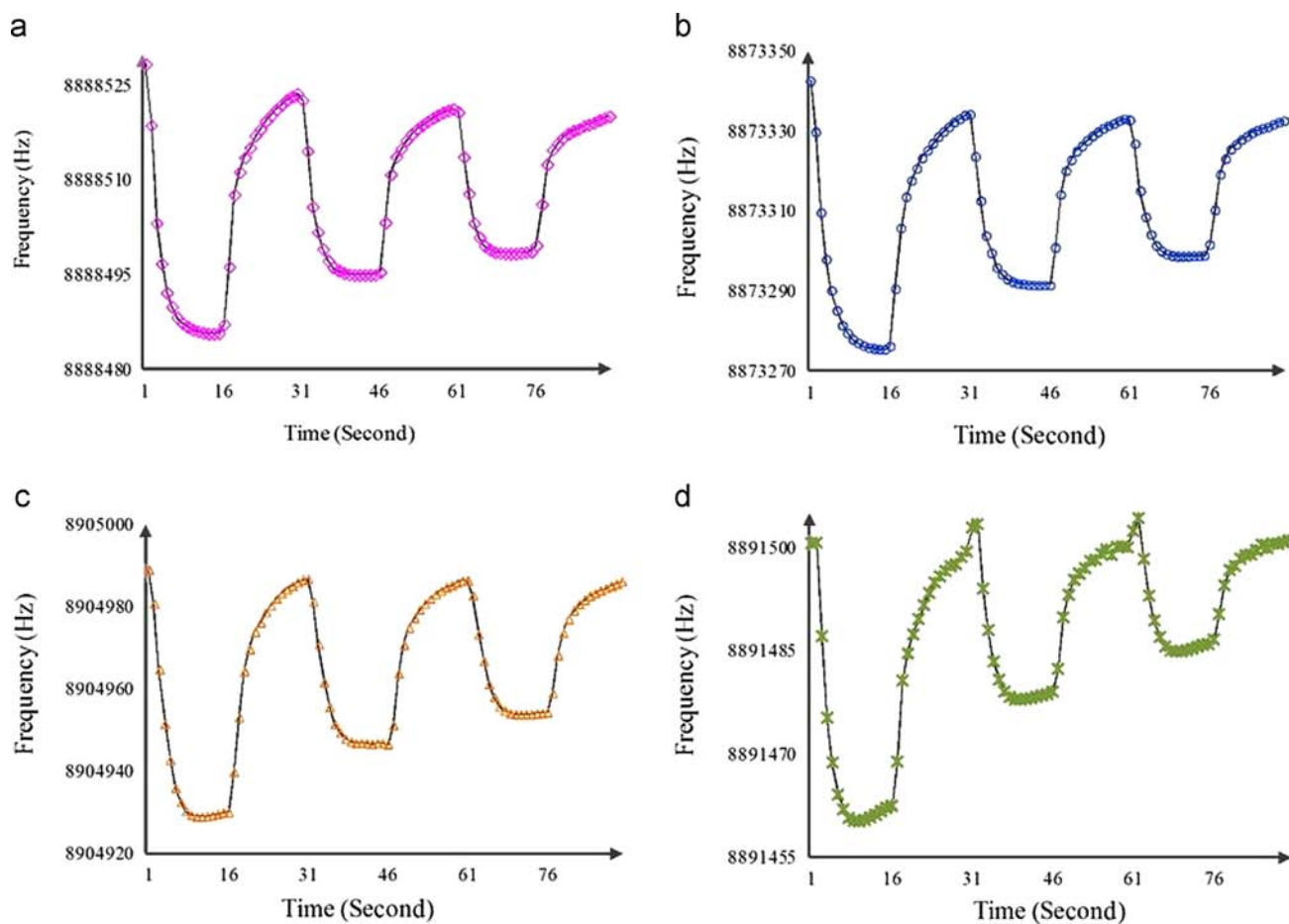


Fig. 6. Response of QCM (a) sensor (S1), (b) sensor (S2), (c) sensor (S3), and (d) sensor (S4) to tertiary mixture of hexanal, heptanal and nonanal (5+5+5  $\mu$ L in glass bottle).

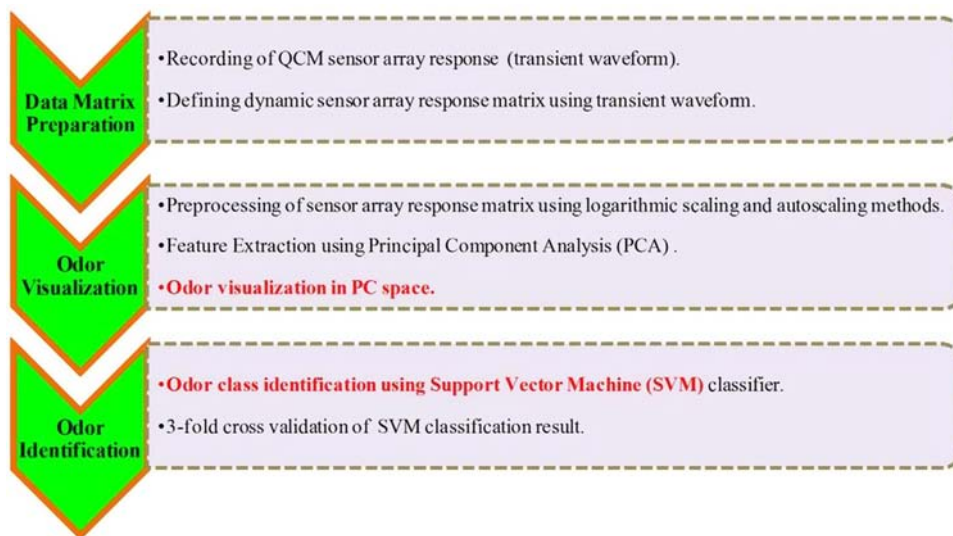


Fig. 7. Sensor array response analysis flow chart.

response to the target aldehyde molecules [54]. Though, the impact of vapor pressure on sensor response was observed in our earlier study [22]. Performance of sensors was evaluated on the basis of sensitivity, baseline drift, and response time. The response time of sensors for single, binary, and tertiary mixtures of aldehyde is discussed separately in last section 3.6. The sensitivity of sensor is

defined as:  $S = \Delta f / \Delta m$ , where  $\Delta f$  is the frequency change due to vapor sorption, and  $\Delta m$  is the mass loading due adsorbed target vapors. Assuming equivalent mass loading of sensors (due to similar amount of MIP coating over QCM surface and alike chemical behavior of three target aldehydes), sensitivity can be redefined as:  $S = c \times \Delta f = c \times (f_b - f_v)$ , where  $c = 1/\Delta m$ ,  $f_b$  is the baseline

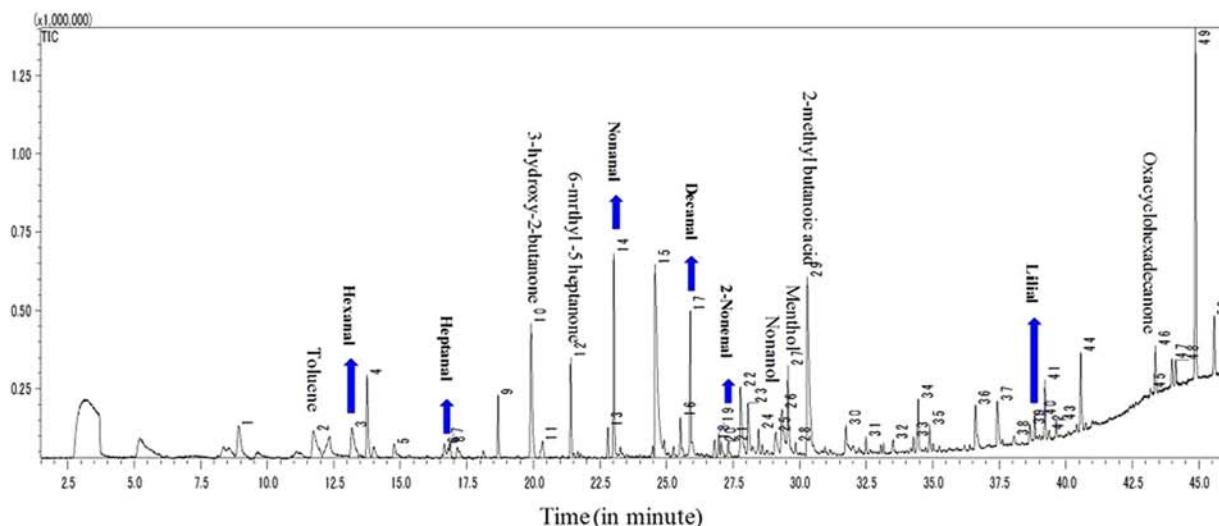


Fig. 8. GC-MS spectra of body odor.

Table 1  
Aldehydes identified in GC-MS spectra of human body odor samples.

Sample source	Detected aldehydes	Peak number	Peak area (in %)	Peak height (in %)
Female left axilla	Hexanal	10	3.75	2.19
	Heptanal	15	0.73	0.81
	Octanal	19	4.94	3.39
	Nonanal	22	8.90	12.1
	Decanal	28	4.93	6.61
Female right axilla	2-Nonenal	31	0.87	1.35
	Hexanal	3	4.32	9.51
	Heptanal	6	0.88	5.13
	Nonanal	15	6.85	2.89
	Decanal	21	3.55	2.95
Female left foot	2-Octenal	39	0.45	0.33
	Hexanal	5	1.50	0.91
	Heptanal	9	0.75	0.58
	Octanal	13	2.56	2.15
	Nonanal	18	8.32	11.6
Female right foot	Decanal	23	3.40	4.62
	Hexanal	15	0.43	0.25
	Decanal	28	0.97	2.53
	Undecanal	31	0.27	0.30
	Hexanal	2	2.00	1.20
Male left axilla	Nonanal	13	6.62	8.38
	Decanal	19	5.10	6.22
	Undecanal	26	0.34	0.46
	Lilial	40	0.56	0.49
	Hexanal	3	1.70	0.98
Male right axilla	Heptanal	6	0.51	0.49
	Nonanal	14	5.15	7.61
	Decanal	17	3.87	5.42
	2-Nonenal	19	0.61	0.85
	Lilial	39	0.64	0.71
Male left foot	Hexanal	2	1.32	0.93
	Nonanal	12	7.55	10.0
	Decanal	18	3.09	4.57
	Hexanal	2	3.92	7.81
	Heptanal	5	1.17	4.59
Male right foot	Nonanal	14	10.2	2.74
	Decanal	21	4.36	2.74
	2-Nonenal	24	0.93	1.21
	2-Undecenal	37	0.26	2.43
	2-Methyl-3-phenylpropanal	39	0.67	0.67

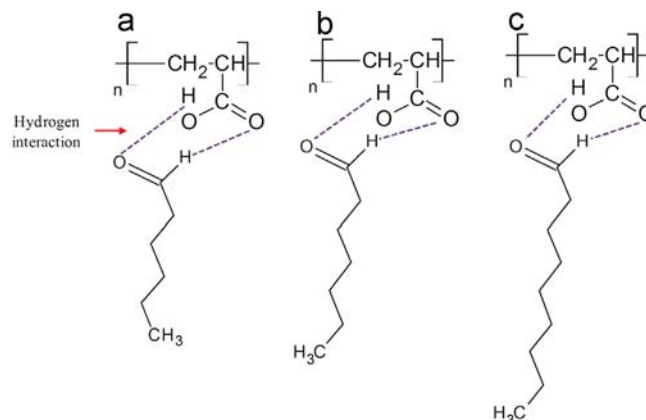


Fig. 9. The presumed interaction between polyacrylic acid (PAA) and target chemicals: (a) hexanal, (b) heptanal and (c) nonanal.

Table 2  
Average response of sensors to single, binary, and tertiary mixtures of aldehydes.

Single aldehyde odor				
Vapor type	Sensor number			
	S1	S2	S3	S4
Hexanal	2.83	7.00	12.66	7.33
Heptanal	13.5	18.33	21.83	8.66
Nonanal	28.5	36.33	41.83	13.66
Binary aldehyde odor				
Hexanal+Heptanal	20.58	26.55	31.36	20.72
Heptanal+Nonanal	34.94	47.08	45.72	19.97
Hexanal+Nonanal	33.22	42.08	43.75	18.30
Tertiary aldehyde odor				
Tertiary odor type-1	25.5	37.5	29.99	10.66
Tertiary odor type-2	27.8	42.0	39.00	13.2
Tertiary odor type-3	23.8	34.6	30.40	12.6

\*Note: sensors response are in Hz. Tertiary odor type-1 is mixture of hexanal=5 $\mu$ L+heptanal=5 $\mu$ L+nonanal=5-30  $\mu$ L (5 $\mu$ L in each steps), Tertiary odor type-2 is mixture of hexanal=5 $\mu$ L+nonanal=5 $\mu$ L+heptanal=10-30  $\mu$ L (5 $\mu$ L in each steps), Tertiary odor type-3 is mixture of heptanal=5 $\mu$ L+nonanal=5 $\mu$ L+hexanal=10-30  $\mu$ L (5 $\mu$ L in each steps).

frequency of QCM, and  $f_v$  is the frequency after the vapor sorption. Sensitivity of sensors was computed using their transient response in 1st measurement cycle.

The baseline drift of sensor is defined as:  $d = (f_{b1} - f_{b2})$ , where  $f_{b1}$ , and  $f_{b2}$  are frequencies of QCM sensor in 1st and 10nd measurement cycles respectively in absence of target chemical



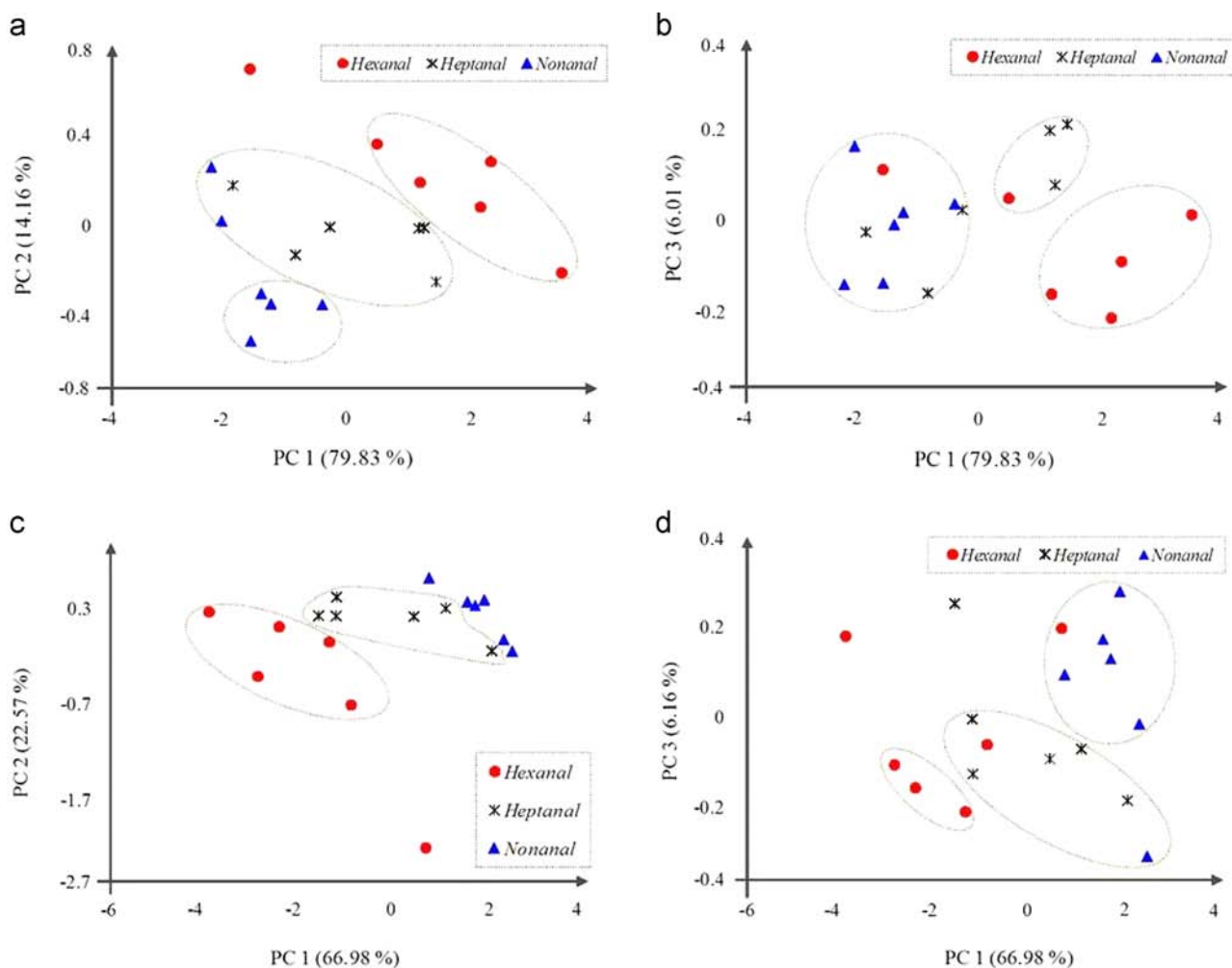


**Fig. 10.** Representation of single aldehydes odor in PC space by QCM sensor array response analysis (excluding sensor-1) in (a) PC 1-PC 2 (b) PC 1-PC 3 directions, and (including sensor-1) in (c) PC 1-PC 2 and (d) PC 1-PC 3 directions.

vapor. The sensitivity values of sensors S1→S4 to nonanal vapor (5  $\mu$ L in glass bottle) are  $S = 49c, 71c, 69c, 46c\text{Hz}/\mu\text{g}$  using the average value of  $f_b$ , and  $f_v$  respectively. The sensitivity value of sensors S1→S4 using the maximum value of  $f_b$ , and  $f_v$  respectively to nonanal vapor are  $S = 77c, 121.3c, 107.3c, 83c\text{Hz}/\mu\text{g}$  (Fig. 4(a)-(d)). These calculated values indicate the highest sensitivity of sensor S2 followed by S3, S1 and S4 to nonanal vapor. The baseline drift values are  $d = 15, 18.3, 12.8, 1.4\text{Hz}$  for sensors S1→S4 respectively. The sensor S3 has baseline drift lower than the sensors S1 and S2. Though the minimum baseline drift is obtained for the sensor S4, which may be due to its lowest sensitivity.

PCA analysis results of sensor array response matrix  $F_s (18 \times 4)$  is shown in Figs. 10(c), and 10(d) in PC 1–2, and PC 1–3 spaces respectively. The three target aldehyde odors are well identified in PC 1–2 space (Fig. 10(c)), except one sample from the hexanal is placed outside its cluster. The partition between the heptanal and nonanal cluster becomes more apparent in PC 1–3 space (Fig. 10(d)). Figs. 10(a) and 10(b) represent the location of three aldehyde odors in PC 1–2 and PC 1–3 spaces respectively, excluding the response of sensor S1 from analysis. It results misclassification of two nonanal samples (identified to heptanal cluster) in PC 1–2 space (Fig. 10(a)). In PC 1–3 space misclassification increases to five, in which one sample of hexanal is assigned to the heptanal and one sample to nonanal cluster (Fig. 10(b)). Thus PCA analysis including response of all the four

sensors result 100% visual identification of single aldehyde odor in PC space.

### 3.3. Sensor array response analysis to binary mixtures of aldehyde odors

Average sensors response to three binary mixtures of aldehyde odors were summarized in Table 2. It is evident that the sensors response to binary mixture of heptanal+nonanal is highest followed by hexanal+nonanal, and hexanal+heptanal. The higher sensor response to first two binary mixtures compared to last one is due to the presence of nonanal in combination. Since all the sensors have maximum response to nonanal vapors. Performance order of sensors to all the three binary mixtures of aldehyde odors almost follow the similar trend as in case of single aldehyde odor, that is,  $S3 > S2 > S1 > S4$  (Fig. 5(a)-(d)). Sensitivities of sensors S1→S4 to binary mixture of hexanal+nonanal (5+5  $\mu$ L in glass bottle) are  $S = 68c, 77c, 70c, 44c\text{Hz}/\mu\text{g}$  using the average and  $S = 96.6c, 129.3c, 102.9c, 83.5c\text{Hz}/\mu\text{g}$  using the maximum values of  $f_b$ , and  $f_v$  respectively (Fig. 5(a)-(d)). The values point out the following sensitivity trends of sensors to the binary mixture of hexanal+nonanal  $S3 > S2 > S1 > S4$ . Baseline drift values for sensors (S1→S4) are  $d = 21.1, 21.3, 9.6, 2.3\text{Hz}$  respectively. Thus baseline drift of sensors are corresponding to the sensors sensitivity to the binary mixtures of aldehyde odor. The sensor S3 has low value of baseline drift compare to sensors S1 and S2, while sensor S4 has its

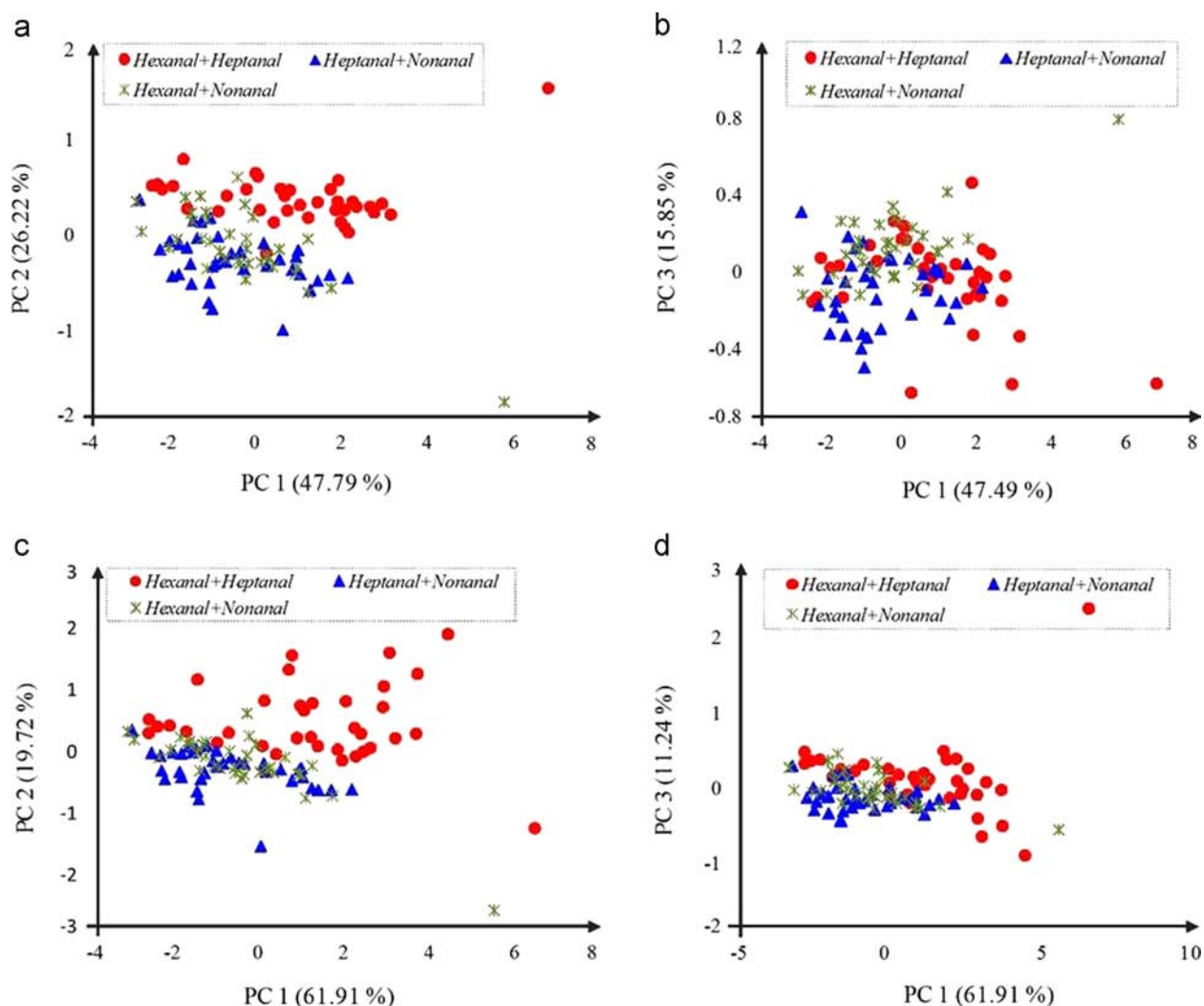


**Fig. 11.** Representation of binary mixture of aldehydes in PC space by QCM sensor array response analysis (excluding sensor-1) in (a) PC 1-PC 2 (b) PC 1-PC 3 directions, and (including sensor-1) in (c) PC 1-PC 2, and (d) PC 1-PC 3 directions.

minimum value. Figs. 11(a)-(d) represent PCA analysis outcomes of sensor array response matrix  $F_m(108 \times 4)$ , in which Figs. 11 (c), and 11 (d) demonstrate the location of three binary mixtures of aldehyde odors in PC 1–2, and PC 1–3 spaces respectively. There is a clear separation between two classes of binary mixtures: hexanal+heptanal, and heptanal+nonanal while the third binary mixture hexanal+nonanal is overlapping with the two other classes of binary mixtures in PC 1–2 space (Fig. 11(c)). The clusters of three classes of binary mixtures further compressed and overlapping increases in PC 1–3 space (Fig. 11(d)). The PC scores plot excluding the response of sensor S1 from analysis is shown in Fig. 11(a) and (b). Compare to Fig. 11(c) the separation between the two classes of binary mixtures: hexanal+heptanal, and heptanal+nonanal becomes more apparent as well the few samples from the third binary mixture hexanal+nonanal are visible in PC 1–2 space (Fig. 11(a)). A slight improvement in between class separation of three binary classes can be seen in PC 1–3 space (Fig. 11(b)), compare to Fig. 11(d). Therefore on the basis of visual discrimination of binary mixture of aldehyde odor, it is clear that the response analysis of three MIP-QCM sensors is more effective in odor recognition. By including the response of non-MIP, the class recognition of binary odor decreases in PC space. To validate this point further SVM classifier is implemented for analysis of PC score matrices  $PC_m(108 \times 3)$  and  $PC_m(108 \times 4)$  of original sensor array response

matrices  $F_m(108 \times 3)$ , and  $F_m(108 \times 4)$  (excluding the response of sensor S1).

For SVM analysis each of PC score matrices were divided into two sets: training and validation set.  $2/3^{\text{rd}}$  of scores (72 samples) were used in training of and remaining  $1/3^{\text{rd}}$  of scores (36 samples) were used for SVM model validation. The SVM model was tuned for kernel functions (linear, polynomial, sigmoid and radial basis) and their allied parameters. Radial basis kernel function based SVM model with  $\gamma = 0.5$  and default value of other parameters result optimum classification in training phase of SVM classifier, same model is used for validation. A 3-fold cross validation approach is adopted to avoid the overtraining and impact of samples on SVM classification outcomes. In this approach SVM model is trained and validated with the three different sets of 72 and 36 PC scores respectively. The class confusion matrix for SVM classifier based on response of three sensors and four sensors are summarized in Table 3. The sub-matrices represent the classification results in 1st, 2nd and 3rd fold of cross validation respectively, in which the three columns stand for the binary mixture of hexanal+heptanal, heptanal+nonanal, and hexanal+nonanal respectively. The emphasized cells in each of the sub-matrices signify the number of binary aldehyde odor correctly recognized to their respective class. Using the PC scores of  $PC_m(108 \times 3)$  in 1st fold of cross validation, there is

**Table 3**  
SVM classification results for three classes of binary mixture of aldehydes.

QCM sensor array response analysis											
Using response of three sensors (S2, S3, S4)					Using response of four sensors (S1, S2, S3, S4)						
I <sup>st</sup> fold											
		Predicted class			No. of properly identified odor			Predicted class			No. of properly identified odor
True class	9	0	3	27	True class	7	0	5	24		
	0	9	3			1	8	4			
	0	3	9			0	3	9			
II <sup>nd</sup> fold											
		Predicted class			No. of properly identified odor			Predicted class			No. of properly identified odor
True Class	11	0	1	24	True Class	11	0	1	24		
	1	5	7			0	5	7			
	3	1	8			3	1	8			
III <sup>rd</sup> fold											
		Predicted class			No. of properly identified odor			Predicted class			No. of properly identified odor
True Class	12	0	0	19	True Class	12	0	0	14		
	0	2	10			0	1	11			
	1	6	5			5	6	1			

confusion amongst the three binary mixtures of aldehyde odors. Three samples from the I<sup>st</sup> binary mixture (hexanal+heptanal) are identified to the II<sup>nd</sup> binary mixture (heptanal+nonanal); three samples from the II<sup>nd</sup> binary mixture are identified to III<sup>rd</sup> binary mixture (hexanal+nonanal); and three samples from the III<sup>rd</sup> binary mixture are identified to I<sup>st</sup> binary mixture. Thus total 27 binary odors are exactly identified to their own class (identification rate 75%). In II<sup>nd</sup> fold the class confusion increase 13, that is, total 24 binary odors are identified correctly (recognition rate 66.67%). In III<sup>rd</sup> fold of cross validation 19 binary odors are recognized correctly (recognition rate 52.77%). Therefore the maximum class recognition rate achieved is 75%. Using the PC scores of  $PC_m(108 \times 4)$ , in I<sup>st</sup> fold of SVM classification, total 24 odors are identified out of 36 (recognition rate 66.67%). In II<sup>nd</sup> and III<sup>rd</sup> Fold total 24 and 14 odors are correctly identified out of 36 respectively. Therefore including the response of all four sensors the maximum class recognition rate is only 66.67%. The SVM classification results (Table 3) and PCA results (Fig. 11(a)–(d)) indicate that the three MIP-QCM sensors are more efficient in recognition of binary mixtures of aldehyde odors, including the response of non-MIP-QCM increases misclassification.

#### 3.4. Sensor array response analysis to tertiary mixture of aldehyde odors

The average value of sensors response to three tertiary mixtures of aldehyde odors were given in Table 2. It is obvious that the maximum sensors response is obtained for the tertiary odor type-2 (hexanal=5  $\mu$ L+nonanal=5  $\mu$ L+heptanal=10–30  $\mu$ L (5  $\mu$ L in each steps)). The sensors response for other two tertiary mixtures: type-1 (hexanal=5  $\mu$ L+heptanal=5  $\mu$ L+nonanal=5–30  $\mu$ L (5  $\mu$ L in each steps)), and type-3 (heptanal=5  $\mu$ L+nonanal=5  $\mu$ L+hexanal=10–30  $\mu$ L (5  $\mu$ L in each steps)) are almost comparable (Table 2). Sensitivity of sensors S1  $\rightarrow$  S4 to tertiary mixture of hexanal, heptanal and, nonanal (5+5+5  $\mu$ L in sampling vial) are  $S = 32c, 46c, 39c, 18cHz/\mu g$  computed from the average values  $f_b$ , and  $f_v$  of and  $S = 42.7c, 66.7c, 66c, 40cHz/\mu g$  using the maximum values of  $f_b$ , and  $f_v$  respectively (Fig. 6(a)–(d)). The following sensitivity trend is obtained to the earlier tertiary mixture of hexanal, heptanal and, nonanal (5+5+5  $\mu$ L)  $S3 \cong S2 > S1 > S4$ . The computed values of baseline drift for sensors S1  $\rightarrow$  S4 to earlier concentration are = 5.7, 10.3, 2.8,

1.2Hz respectively. The values of baseline drift are in according with the sensitivity of sensors. As the baseline drift of sensor S3 has lower value than the sensors S1 and S2. Minimum value of baseline drift is obtained for the sensor S4. Figs. 12(a)–(d) present PCA analysis results of sensor array response matrix  $F_t(16 \times 4)$ . Figs. 12(c) and 12(d) exhibit the position of three tertiary mixtures of aldehyde odors in PC 1–2 and PC 1–3 spaces respectively. There is a clear partition between two classes of tertiary mixtures type-1 and type-2, third tertiary mixture type-3 is overlapping with the rest two tertiary mixture types in PC 1–2 space (Fig. 12(c)). Two odor samples are misclassified as well three are laying outside the clusters. The compactness of odor clusters increases in PC 1–3 space (Fig. 12(d)). Four odor samples are misclassified and five are lying outside the clusters. Fig. 12(a) presents the tertiary odors in PC 1–2 space excluding the response of sensor S1 from analysis. In this case two odor samples are misclassified and three are lying outside the cluster. This result is similar to the PC score plot in Fig. 12(c). Likewise representation of tertiary odor in PC 1–3 space excluding the response of sensor S1 from analysis is shown in Fig. 12(b) in which four odor samples are misclassified and five are laying outside the odor clusters. This result is identical to the PC score plot in Fig. 12(d). Consequently, the PC score plots shown in Fig. 12(a)–(d) conclude that there is no improvement in visual class recognition of tertiary odors in PC spaces after including the response of non-MIP-QCM sensor in analysis. Sensors response decreases between subsequent exposures to sample vapours (Figs. 4–6). This is due to decrease in exposed chemical vapor concentration in subsequent cycles. Since as time passes, the vapor concentration of target chemical in sampling glass vial decrease.

#### 3.5. Combined analysis of sensor array response to single, binary, and tertiary mixtures of aldehyde odors

To recognize the single, binary, and tertiary aldehyde odors simultaneously in presence of each other, the three sensors response matrices  $F_s(18 \times 4)$ ,  $F_b(108 \times 4)$  and  $F_t(16 \times 4)$  were combined and used for further analysis with the PCA and SVM methods. Figs. 13(a)–(d) exhibit the PCA analysis outcomes of combined sensors response matrix. The position of single aldehyde odor, three classes of binary mixtures of aldehyde odors, and tertiary mixture of aldehyde odors using the response analysis of three

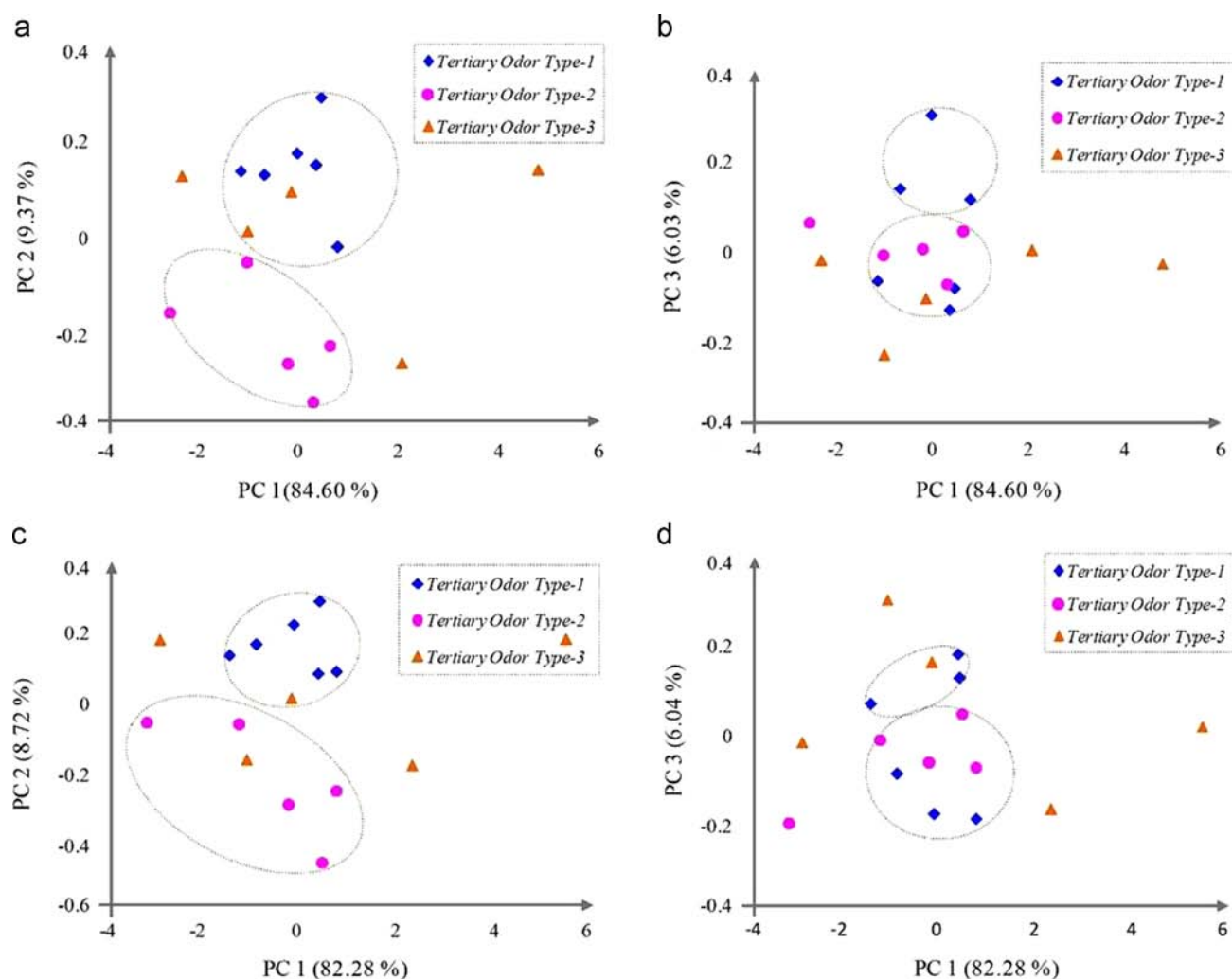


**Fig. 12.** Representation of tertiary mixture of aldehydes in PC space by QCM sensor array response analysis (excluding sensor-1) in (a) PC 1-PC 2 (b) PC 1-PC 3 directions, and (including sensor-1) in (c) PC 1-PC 2, and (d) PC 1-PC 3 directions.

MIP-QCM sensors is shown in Fig. 13(c). It is evident that except the binary odor type-3 (hexanal+nonanal), rest four odor classes are partially overlapping, however a complete separation is observed between the single and tertiary odor classes, single and binary odor type-2 (heptanal+nonanal), binary odor type-1 (hexanal+heptanal) and type-2, and binary odor type-1 and tertiary odor. Including the response of non-MIP QCM sensor, the PCA analysis result is shown in Fig. 13(d). On the basis of visual inspection, it is clear that the overlapping increases amongst the binary odor type-1, type-2, and tertiary odor compare to Fig. 13(c). Thus including the response of non-MIP QCM sensor in analysis is not appropriate. Further the three binary mixtures classes of aldehyde odor are combined together in one class, after that the sensors response matrix is analyzed and PCA outcomes are shown in Fig. 13(a) excluding the response of non-MIP QCM sensor, and in Fig. 13(b) after including the response of non-MIP QCM sensor. Compare to Fig. 13(b) better separation amongst the single, binary, and tertiary aldehyde odors is observed in Fig. 13(a). Particularly partitions of binary aldehyde odors with the single and tertiary odors are more obvious. Results again confirm minor contribution of non-MIP QCM sensor response in analysis outcome. This point is further verified with quantitative identification of single, binary, and tertiary odors simultaneously using SVM classifier. For SVM classification the PC score matrices ( $\mathbf{PC}_s (18 \times 4)$ ,  $\mathbf{PC}_m (108 \times 4)$  and  $\mathbf{PC}_t (16 \times 4)$  of original sensors response matrices ( $\mathbf{F}_s (18 \times 4)$ ,  $\mathbf{F}_b (108 \times 4)$

and  $\mathbf{F}_t (16 \times 4)$ ) were combined. The binary mixtures classes are assumed as a single class. The combined PC score matrix is divided into training and validation sets. About 2/3<sup>rd</sup> of scores (total 95 samples: 12 from single odor class, 72 from binary mixture odor class, and 11 from tertiary mixture odor class) were used for training and rest 1/3<sup>rd</sup> of scores (total 47 odor samples: 6 from single odor class, 36 from binary mixture odor class, and 5 from tertiary mixture odor class) were used for validation of SVM model. After tuning, for kernel function and their related parameters optimized SVM model was used for classification (Similar to SVM model used in Section 3.3). The class confusion matrices by excluding, and including the response of non-MIP QCM sensor are given in Table 4. Using the response of three MIP-QCM sensors in 1st fold, all the aldehyde odors from the binary mixture classes are correctly identified, however the 6 samples from the single odor class and 5 samples from the tertiary odor class were identified to the binary odor class (class recognition rate 76.60%). In 2nd fold the class confusion decreases, resulting identification of 39 odors correctly to their respective class (recognition rate 82.98%. Though maximum class confusion can be seen in the 3rd fold, in which only 15 samples are correctly identified. After excluding the response of non-MIP QCM sensor from analysis result maximum recognition rate 82.98%. Although including them in analysis, SVM classifier results 100% recognition of odors from binary mixtures of aldehyde, however the single and tertiary aldehyde odors have recognition rate 76.60% only in 1st fold. In 2nd and 3rd fold 20 and

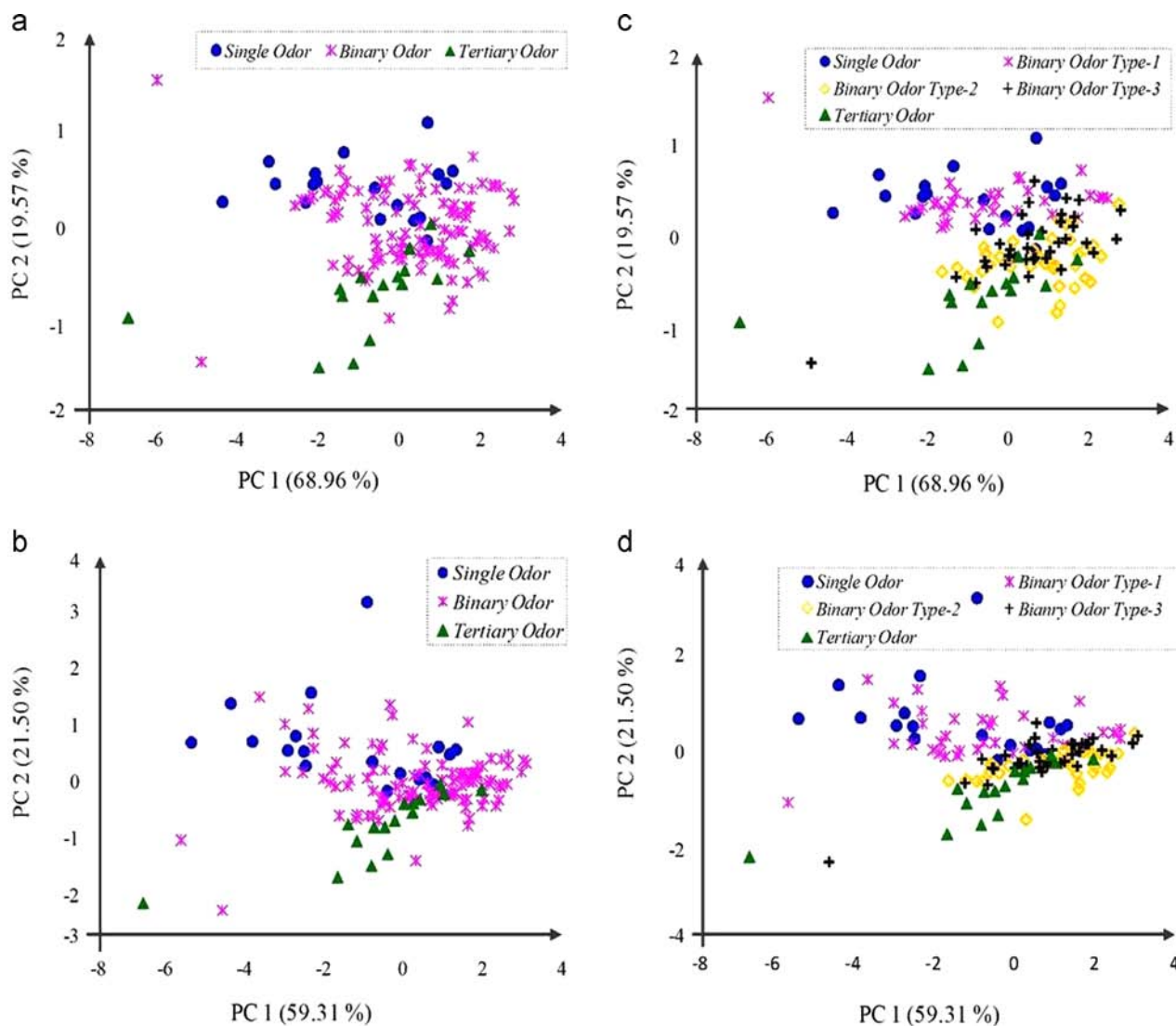


**Fig. 13.** Representation of aldehydes in PC space combining three classes of binary odors into one class in PC 1-PC 2 directions with response analysis of (a) three sensors, (b) four sensors, and using three separate classes of binary odors with response analysis of (c) three sensors, (d) four sensors.

34 samples are correctly identified respectively. The maximum class recognition rate in this case is 76.60%, which is less than the maximum class recognition rate 82.98% of previous case (excluding the response of non-MIP QCM sensor). It is equivalent to the PCA results in Fig. 13 (a)–(d).

Characterization result (Fig. 8, Table 1) of body odor samples indicates the presence of organic acids, aldehydes, and ketones, etc as the major chemical classes, due to this in our earlier study [22] we have reported the MIP-QCM sensors for the detection of three organic acids singly and in their mixtures. Likewise in present study we target the identification of three aldehydes identified in real samples of body odor in singly and in mixtures. As if we can develop the MIP-QCM sensors for identification of chemicals from major functional groups found in real body odor such as acid, aldehyde, ketone in singly and in mixtures then we can also use similar sensing system for body odor recognition in real scenario. Since body odor is the complex composition of chemicals from major functional groups with other interferents. In our future study, we target identification of other major chemical classes in body odor using the similar MIP-QCM sensing system and later on test this system for differentiation of body odor in real scenario.

### 3.6. Response (adsorption) and recovery (desorption) time of sensors to aldehyde odors

Sensors S2 and S3 are most sensitive to the aldehyde odors (Figs. 4–6). A schematic calculation of their response time ( $t_{on}$ ) and recovery time ( $t_{off}$ ) according to definition in Ref. [30] is given in Fig. 14 (a)–(d). Particularly, Fig. 14 (a) represents the response of sensor S2 to heptanal vapors ( $5\mu\text{L}$  in glass bottle). Full response of sensor S2 is 84.6 Hz and time required to read the 90% of full response 76.14 Hz is ( $t_{on}$ ) 10 s. Also the time required to recover the baseline ( $t_{off}$ ) is 13 s. Similarly Fig. 14(b)–(d) demonstrate the response of sensor S2 to binary odor generated with hexanal+heptanal mixture ( $5+5\mu\text{L}$  in glass bottle) with response time 11 s and recovery time 12 s, response of sensor S3 to binary odor generated with heptanal+nonanal mixture ( $5+5\mu\text{L}$  in glass bottle) with response time only 5 s and recovery time 12 s and response of sensor S3 to tertiary odor generated with hexanal+heptanal+nonanal ( $5+5+5\mu\text{L}$  in glass bottle) with response time 5 s and recovery time 12 s respectively. It is obvious that the sensor S3 response faster than the S2. Sensor response time and recovery time depend on chemical behavior of MIP film and target chemical molecule as well concentration of latter. We

**Table 4**  
SVM classification results for single, binary, and tertiary mixtures of aldehyde odors (assuming all the three classes of binary mixtures as a single class).

QCM sensor array response analysis				
Using response of three sensors (S2, S3, S4)				
I <sup>st</sup> fold				
Predicted class		No. of properly identified odor		
True class	0	6	0	36
	0	36	0	
	0	5	0	
II <sup>nd</sup> fold				
Predicted class		No. of properly identified odor		
True Class	2	4	0	39
	0	36	0	
	0	4	1	
III <sup>rd</sup> fold				
Predicted class		No. of properly identified odor		
True Class	1	0	0	15
	23	12	1	
	0	3	2	
Using response of four sensors(S1, S2, S3, S4)				
I <sup>st</sup> fold				
Predicted class		No. of properly identified odor		
True class	0	6	0	36
	0	36	0	
	0	5	0	
II <sup>nd</sup> fold				
Predicted class		No. of properly identified odor		
True Class	0	6	0	20
	18	18	0	
	0	3	2	
III <sup>rd</sup> fold				
Predicted class		No. of properly identified odor		
True Class	0	6	0	34
	0	31	5	
	0	2	3	

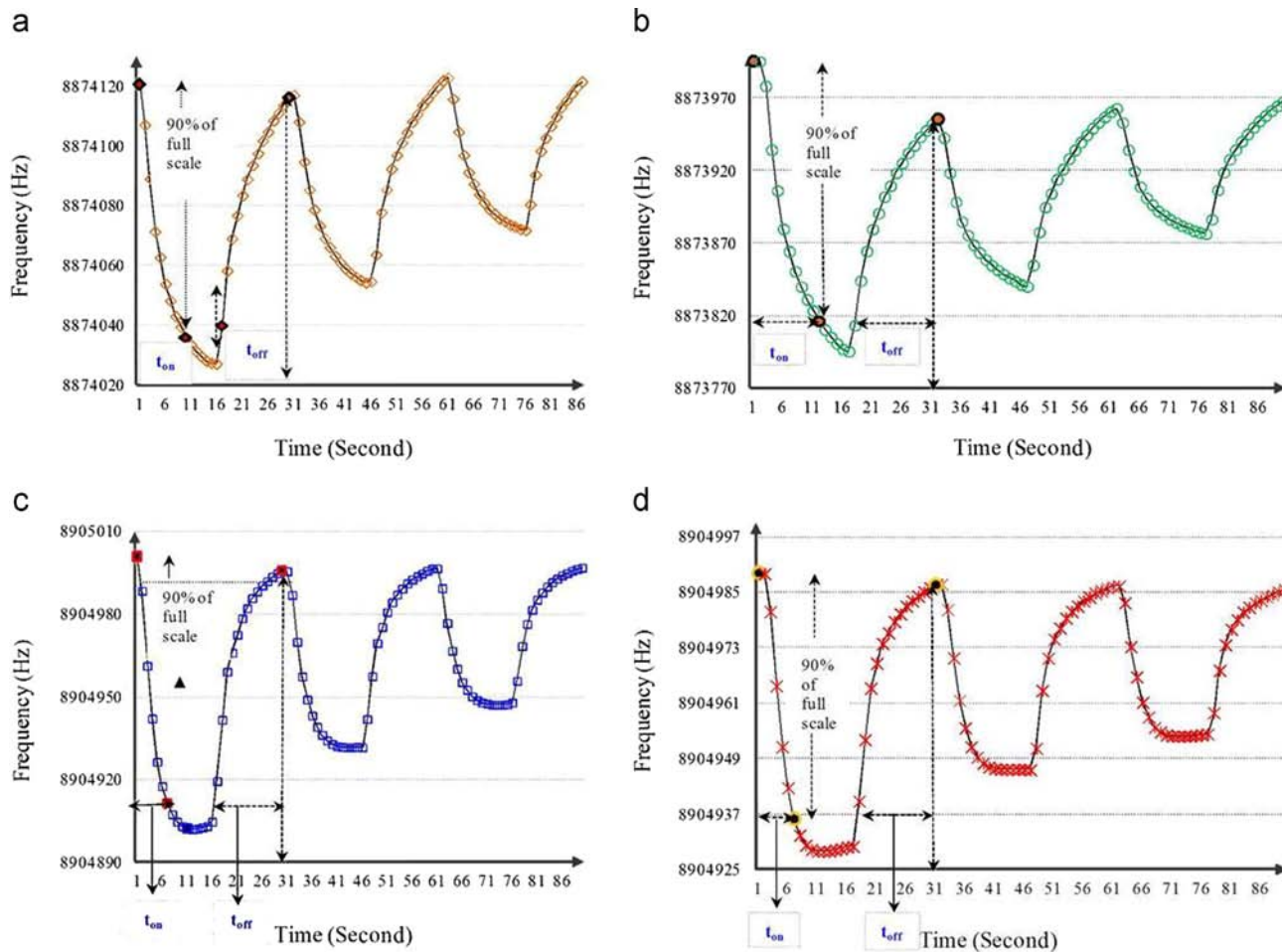


**Fig. 14.** Response time of MIP coated QCM sensor to (a) heptanal vapors (5  $\mu$ L in sampling vial), (b) binary mixture of hexanal and heptanal (5+5  $\mu$ L in glass bottle), (c) binary mixture of heptanal and nonanal (5+5  $\mu$ L in glass bottle), and (d) tertiary mixture of hexanal, Heptanal and nonanal (5+5+5  $\mu$ L in glass bottle).

hardly noticed the reported value of QCM sensor response time for single and mixed odors of aldehydes. Though some reported values of QCM sensor response time and recovery time for other vapors are as follows: 48 s and 91 s for water vapor [44], 6 s and 27 s for acetic acid vapor [48], average response time 90 s for acetone vapors [55], etc. According to Gardener et al. [30,56]  $t_{on}$  should be few seconds and sum of  $t_{on} + t_{off}$  should be 1–2 minutes. MIP-QCM sensors in present study succeed to achieve this limit by which quick identification of aldehyde odors singly, binary, and tertiary mixtures is feasible both independently and simultaneously.

#### 4. Conclusions

A novel acids template molecule based MIP coated QCM sensor array has been developed for the detection of three biomarker aldehydes in body odor. The presence of target aldehydes was confirmed with the SPME-GC-MS analysis of real body odor samples. The target aldehyde odors were identified in singly, binary, and tertiary mixtures independently as well in combination. The hexanoic acid template molecule based MIP coated QCM sensor exhibit quick response ( $t_{on}=5$  s) and high selectivity and reversibility compare to other sensors. The aldehyde odors were effectively identified in PC space as well with SVM classifier. Future work will be concerned to the development of aldehyde template molecules based MIP coated QCM sensors for effective recognition of additional saturated and branched aldehydes in their binary and tertiary mixtures in presence of other interfering vapors.

#### Acknowledgments

This research work was supported by Grant-in-Aid for JSPS fellows 24.02367 and partly by JSPS KAKENHI Grant no. 25420409. The author S.K.J. gratefully acknowledges Dr. C. Liu, lab colleagues, Mrs. Anju Sunil Jha for their contribution and support during the study, and distinguished reviewers for their valuable comments and suggestions.

#### References

- [1] S.K. Pandey, K. Kim, *Trend Anal. Chem.* 30 (2011) 784–796.
- [2] S. Yamazaki, K. Hoshino, M. Kusuhara, *Anti-Aging Med* 7 (2010) 60–65.
- [3] G. Preti, J.J. Leyden, *J. Invest. Dermatol.* 130 (2010) 344–346.
- [4] D.J. Penn, E. Oberzaucher, K. Grammer, G. Fischer, H.A. Soini, D. Wiesler, M.V. Novotny, S.J. Dixon, Y. Xu, R.G. Brereton, *J. R. Soc. Interface* 4 (2007) 331–340.
- [5] R.M.S. Thorn, J. Greenman, *J. Breath Res* 6 (2012) 024001.
- [6] J. Havlicek, P. Lenochova, *Chem. Senses* 31 (2006) 747–752.
- [7] L. Fang, G. Clausen, P.O. Fanger, *Indoor Air* 8 (1998) 80–90.
- [8] A. D'Amico, C.D. Natale, R. Paolesse, A. Macagnano, E. Martinelli, G. Pennazza, M. Santonic, M. Bernabei, C. Roscioni, G. Galluccio, R. Bono, E.F. Agro, S. Rullo, *Sens. Actuat. B-Chem.* 130 (2008) 458–465.
- [9] M. Statheropoulos, C. Spiliopoulou, A. Agapiou, *Foren. Sci. Int.* 153 (2005) 147–155.
- [10] A.K. Jain, T., *IEEE, Circ. Syst. Vid.* 14 (2004) 4–20.
- [11] P.A. Lafleur, L.G. Pertson, *US Patent 5780020 A* (1998) 1–12.
- [12] S. Haze, Y. Gozu, S. Nakamura, Y. Kohno, H. Sawano, K. Ohta, K. Yamazaki, *J. Invest. Dermatol.* 116 (2001) 520–524 (2001).
- [13] U.R. Bernier, M.M. Booth, R.A. Yost, *Anal. Chem.* 71 (1999) 1–7.
- [14] U.R. Bernier, D.L. Kline, D.R. Barnard, C.E. Schreck, R.A. Yost, *Anal. Chem.* 72 (2000) 747–756 (2000).
- [15] S. Munk, P. Munch, L. Stahnke, J. Adler-Nissen, P. Schieberle, *J. Surfact. Deterg.* 3 (2000) 505–515.
- [16] P. Martinez-Lozano, J.F. Mora, *Anal. Chem.* 80 (2008) 8210–8215.
- [17] N. Goetz, G. Kaba, D. Good, G. Hussler, P. Bore, *J. Soc. Cosmet. Chem.* 39 (1988) 1–13.
- [18] M. Kubota, R. Komaki, Y. Ito, M. Arai, H. Niwase, *J. Soc. Cosmet. Chem.* 28 (1994) 295–298.
- [19] L. Dormont, J. Bessiere, D. McKey, A. Cohuet, *J. Exp. Bio.* 216 (2013) 2783–2788.
- [20] C. Liu, Y. Furusawa, K. Hayashi, *Sens. Actuat. B-Chem.* 183 (2013) 117–123.
- [21] S.K. Jha, M. Imahashi, K. Hayashi, T. Takamizawa, *Proceedings of IEEE-ISSNIP Singapore* (2014) 1–6 (DOI: 978-1-4799-2843-9/14).
- [22] S.K. Jha, C. Liu, K. Hayashi, *Sens. Actuat. B-Chem.* 204 (2014) 74–87.
- [23] M. Gallagher, C.J. Wysocki, J.J. Leyden, A.I. Spielman, X. Sun, G. Preti, *Brit. J. Dermatol.* 159 (2008) 780–791.
- [24] X.N. Zeng, J.J. Leyden, H.J. Lawley, K. Sawano, I. Nohara, G. Preti, *J. Chem. Ecol.* 17 (1991) 1469–1491.
- [25] C.D. Natale, A. Macagnano, R. Paolesse, E. Tarizzo, A. Mantini, A. D'Amico, *Sens. Actuat. B-Chem* 65 (2000) 216–219.
- [26] C. Wongchoosuk, M. Lutz, T. Kerdcharoen, *Sensors* 9 (2009) 7234–7249.
- [27] S.K. Jha, R.D.S. Yadava, *Sens. Lett.* 9 (2011) 1612–1622.
- [28] E.J. Staples, *Proceedings of the 92nd Air & Waste Management Meeting St. Louis, June* (1999) 4093–4101.
- [29] G. Sauerbrey, *Zeitschrift für Physik* 155 (1959) 206–222.
- [30] J.W. Gardener, P.N. Bartlett, *Electronic Noses: Principles and Applications*, Oxford University press, New York, 1999.
- [31] S.K. Vashist, P. Vashist, *J. Sensors* (2011) 1–13.
- [32] K.A. Marx, *Macromol.* 4 (2003) 1099–1120.
- [33] K. Arshak, E. Moore, G.M. Lyons, J. Harris, S. Clifford, *Sens. Rev.* 24 (2004) 181–198.
- [34] G. Barko, J. Hlavay, *Talanta* 44 (1997) 2237–2244.
- [35] X. Xu, H. Cang, C. Li, Z.K. Zhao, H. Li, *Talanta* 78 (2009) 711–716.
- [36] M. Avila, M. Zougagh, A. Escarpa, A. Rios, *Talanta* 72 (2007) 1362–1369.
- [37] K. Haupt, K. Mosbach, *Chem. Rev.* 100 (2000) 2495–2504.
- [38] C.J. Percival, S. Stanley, M. Galle, A. Braithwaite, M.I. Newton, G. McHale, W. Hayes, *Anal. Chem.* 73 (2001) 4225–4228.
- [39] M. Matsuguchi, T. Uno, *Sens. Actuat. B-Chem* 113 (2006) 94–99.
- [40] A. Gultekin, G. Karanfil, M. Kus, S. Sonmezoglu, R. Say, *Talanta* 119 (2014) 533–537.
- [41] I. Bakas, N.B. Oujji, G. Istamboulie, S. Piletsky, E. Piletska, E. Ait-Addi, I. Ait-Ichou, T. Noguier, R. Rouillon, *Talanta* 125 (2014) 313–318.
- [42] M.L. Yola, L. Uzun, N. Ozaltin, A. Denizli, *Talanta* 120 (2014) 318–324.
- [43] A. Mirmohseni, V. Hassanzadeh, *J. Appl. Polym. Sci.* 79 (2001) 1062–1066.
- [44] Y. Sun, R. Wu, Y. Huang, P. Su, M. Chavali, Y. Chen, C. Lin, *Talanta* 73 (2007) 857–861.
- [45] B. Mumyakmaz, A. Ozmen, M.A. Ebeoglu, C. Tasaltin, I. Gurol, *Sens. Actuat. B-Chem.* 147 (2010) 277–282.
- [46] S.K. Jha, R.D.S. Yadava, *IEEE Sens. J.* 9 (2009) 1202–1208.
- [47] R.G. Osuna, H.T. Nagle, *IEEE Trans. Syst. Man. Cybern. B* 29 (1999) 626–632.
- [48] L.I. Smith, *A tutorial on principal components analysis* (2002) 1–26 [http://www.cs.otago.ac.nz/cosc453/student\\_tutorials/principal\\_components.pdf](http://www.cs.otago.ac.nz/cosc453/student_tutorials/principal_components.pdf).
- [49] C.M. Bishop, *Pattern Recognition and Machine Learning*, Springer, New York, 2006.
- [50] R Development Core Team, *R: A language and environment for statistical computing*. R Foundation for statistical computing, Vienna, Austria, (<http://www.R-project.org>), 2008.
- [51] V. Vapnik, *Estimation of Dependences Based on Empirical Data*, Springer, New York, 1982.
- [52] J.C. Christopher, A. Burges, *Data Min. Knowl. Disc* 2 (1998) 121–167.
- [53] E. Dimitriadou, K. Hornik, F. Leisch, D. Meyer, A. Weingessel, A. e1071: *Misc Functions of the Department of Statistics (e1071)*, TU Wien, R package version 1 (2008) Vienna, Austria, 5–18.
- [54] D.R. Lide, *Handbook of Chemistry and Physics*, CRC Press, Florida, USA, 2004.
- [55] H. Huang, J. Zhou, S. Chen, L. Zeng, Y. Huang, *Sens. Actuat. B-Chem* 101 (2004) 316–321.
- [56] A.S. Yuwono, P.S. Lammers, *J. Sci. Res. Dev.* 3 (2004) 9–25.